

Effective slip over superhydrophobic surfaces in thin channels

François Feuillebois,¹ Martin Z. Bazant,^{1,2,3} and Olga I. Vinogradova^{1,4,5}

¹*CNRS UMR 7636 and 7083, ESPCI, 10 rue Vauquelin, 75005 Paris, France*

²*Department of Mathematics, Massachusetts Institute of Technology, Cambridge, MA 02139 USA*

³*Department of Mechanical Engineering, Stanford University, Stanford, CA 94305 USA*

⁴*A.N. Frumkin Institute of Physical Chemistry and Electrochemistry, Russian Academy of Sciences, 31 Leninsky Prospect, 119991 Moscow, Russia*

⁵*ITMC and DWI, RWTH Aachen, Pauwelsstr. 8, 52056 Aachen, Germany*

(Dated: October 31, 2018)

Superhydrophobic surfaces reduce drag by combining hydrophobicity and roughness to trap gas bubbles in a micro- and nanoscopic texture. Recent work has focused on specific cases, such as striped grooves or arrays of pillars, with limited theoretical guidance. Here, we consider the experimentally relevant limit of thin channels and obtain rigorous bounds on the effective slip length for any two-component (e.g. low-slip and high-slip) texture with given area fractions. Among all anisotropic textures, parallel stripes attain the largest (or smallest) possible slip in a straight, thin channel for parallel (or perpendicular) orientation with respect to the mean flow. For isotropic (e.g. chessboard or random) textures, the Hashin-Strikman conditions further constrain the effective slip. These results provide a framework for the rational design of superhydrophobic surfaces.

PACS numbers: 83.50.Rp, 47.61.-k, 68.08.-p

Introduction.— The design and fabrication of micro- and nanotextured surfaces have received much attention in recent years. It has also been recognized that a modified surface profile can induce novel wetting properties of a solid, which could not be achieved without roughness [1]. Depending on interfacial characteristics, the Wenzel state, where the liquid impregnates the surface, can enhance wettability, or the Cassie state, where the texture is filled with gas, can dramatically amplify hydrophobicity [2]. The remarkable mobility of liquids on such superhydrophobic surfaces renders them “self-cleaning” and causes droplets to roll (rather than slide) under gravity and rebound (rather than spread) upon impact. Beyond their fundamental interest, superhydrophobic surfaces may revolutionize microfluidics [3, 4], by reducing viscous drag in very thin channels and amplifying transport phenomena [5] and transverse flows [6].

Reduced wall friction is associated with the breakdown of the no-slip hypothesis. It has recently become clear that liquid slippage occurs at smooth hydrophobic surfaces, as described by the Navier boundary condition [7, 8, 9] $v_s = b\partial v/\partial z$, where v_s is the slip (tangential) velocity at the wall and the axis z is normal to the surface. A mechanism for dramatic friction reduction involves a lubricating gas layer of thickness δ with viscosity μ_g much smaller than that of the liquid μ [10], so that $b \approx \delta(\mu/\mu_g - 1) \approx 50\delta$ [11]. This scenario allows to achieve slip length of only of a few tens of nm in case of smooth hydrophobic surfaces [12]. The presence of a rough texture however stabilizes the gas layer, and by increasing its height δ , the slip length may reach tens of μm over the gas regions. The composite nature of the texture, however, requires regions of lower slip (or no slip) in direct contact with the liquid, so the effective slip length of the surface b^* (defined below) is reduced.

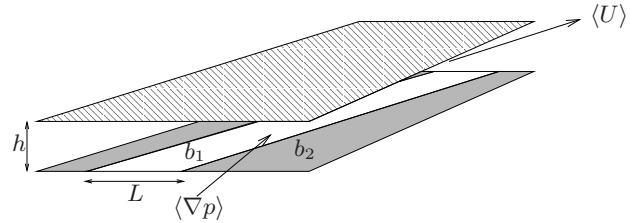


FIG. 1: Sketch of a thin channel, where the gap width h is small compared with the texture characteristic length L .

For anisotropic textures b^* depends on the flow direction and is generally a tensor [13]. Indeed, experimental studies of flow past superhydrophobic surfaces suggest that b^* does not exceed several μm [14] and varies with the orientation of the wall texture relative to flow [15].

The quantitative understanding of liquid slippage past superhydrophobic surfaces is still challenging, and little theoretical guidance is available for the design of optimal textures. Some exact solutions are known for a flow on alternating (parallel or transverse) no-slip and perfect slip stripes [16, 17, 18] or transverse inhomogeneous slip sectors [19]. Simplified scaling expressions have been proposed for a geometry of pillars [9, 20], and numerical approaches have also been followed [21, 22, 23]. Nevertheless, general principles to maximize or minimize the effective slip have not yet been established, even in the simple (but experimentally relevant) lubrication limit, where the implication of slip is the most pronounced [10].

In this Letter, we propose a systematic approach to optimize the effective slip length of a superhydrophobic surface in a thin channel, based on the theory of heterogeneous porous materials [24, 25]. We derive rigorous bounds on the effective slip length for arbitrary

anisotropic or isotropic textures, depending only on the area fractions and local (any) slip lengths of the high-slip and low-slip regions. In some cases, the bounds are close enough to render detailed calculations unnecessary, and in others the theory provides optimal textures which attain the bounds (notably the maximum possible effective slip). Our theory also predicts b^* in certain geometries without requiring any calculation.

Model and analysis.— We consider pressure-driven flow of a viscous fluid between two textured parallel plates (“+” and “-”) separated by h , as sketched in Fig. 1. Motivated by superhydrophobic surfaces in the Cassie state, we assume flat interfaces (such as idealization has been used in most of previous studies [16, 21] and corresponds to a minimum dissipation in the system [18, 26]) characterized by spatially varying slip lengths $b^+(x, y)$ and $b^-(x, y)$. Our analysis is based on the lubrication (or Hele-Shaw) limit of a thin channel, where the texture varies over a scale $L \gg h$; the flow profile is then locally parabolic at any position.

To evaluate the effective slip length, we calculate the velocity profile and integrate it across the channel to obtain the depth-averaged velocity \mathbf{U} in terms of the pressure gradient ∇p along the plates. As usual for the Hele-Shaw cell, the result may be written as a Darcy law

$$\mathbf{U} = -\frac{k(x, y)}{\mu} \nabla p, \quad (1)$$

where we obtain the permeability

$$k(x, y) = \frac{h^2}{12} \left(1 + \frac{3(\beta^+ + \beta^- + 4\beta^+\beta^-)}{1 + \beta^+ + \beta^-} \right)$$

in terms of the normalized slip lengths $\beta^+ = b^+(x, y)/h$ and $\beta^- = b^-(x, y)/h$. The permeability is maximized with two equal surfaces, $\beta^+ = \beta^- = \beta(x, y)$, so we consider this case (II) with the goal of minimizing drag. We also consider the case (I) of one no-slip wall ($\beta^+ = \beta(x, y); \beta^- = 0$), which is relevant for various setups, where the alignment of opposite textures is inconvenient or difficult. The permeability then takes the form:

$$k(x, y) = \frac{h^2}{12} \begin{cases} 1 + 3\beta(x, y)/[1 + \beta(x, y)] & \text{case (I)} \\ 1 + 6\beta(x, y) & \text{case (II)} \end{cases} \quad (2)$$

In general, the slip length may also vary locally with orientation, so that $b(x, y)$ becomes a second-rank tensor $\mathbf{b}(x, y)$, from which a tensorial permeability $\mathbf{k}(x, y)$ can be derived [13].

The slip length $b(x, y)$ (or $\mathbf{b}(x, y)$) varies on the microscale $L \gg h$, but we are interested in properties of the flow at the macroscale. A natural definition of the effective slip length is based on a hypothetical uniform channel with the same effective permeability. First, we average (1) over the texture (denoted by $\langle \cdot \rangle$) at a mesoscale

that is smaller than the macroscale, but much larger than L , to obtain

$$\langle \mathbf{U} \rangle = -\frac{1}{\mu} \langle k(x, y) \nabla p \rangle = -\frac{\mathbf{k}^*}{\mu} \cdot \langle \nabla p \rangle$$

where in the last step we introduce the effective permeability \mathbf{k}^* , which is generally a tensor, even if $k(x, y)$ is locally isotropic. Only with an isotropic structure at the mesoscale does it become a scalar k^* . This definition is subject to the boundary condition of a uniform pressure gradient ∇P applied at the macroscale, which must equal the average pressure gradient, $\langle \nabla p \rangle = \nabla P$, since the pressure is harmonic [24].

By analogy with (2), we define the effective slip length in terms of the effective permeability:

$$k_j^* = \frac{h^2}{12} \begin{cases} 1 + 3\beta_j^*/[1 + \beta_j^*] & \text{case (I)} \\ 1 + 6\beta_j^* & \text{case (II)} \end{cases} \quad (3)$$

where the principal (eigen)directions $j = 1, 2$ of \mathbf{k}^* correspond with those of $\beta^* = \mathbf{b}^*/h$, where \mathbf{b}^* is the effective slip length tensor [13].

Motivated again by superhydrophobic surfaces in the Cassie state, we assume $b(x, y)$ switches between two values, b_1 and b_2 , associated with permeabilities k_1, k_2 from (2), for regions (or “phases”) of liquid-solid and liquid-gas interfaces, respectively. Let ϕ_1 and ϕ_2 be the area fractions of the two phases with $\phi_1 + \phi_2 = 1$. We make no further assumptions in deriving bounds on the effective slip length β^* in a principal direction (without transverse flow), aside from distinguishing between anisotropic and isotropic textures.

Anisotropic textures.— In the general case of an orientation-dependent texture ($\mathbf{k}^* \neq k^*\mathbf{I}$), the Wiener bounds apply for the effective permeability in a given direction [25]: $k^\perp \leq k^* \leq k^\parallel$. The lower bound k^\perp can be attained by parallel stripes perpendicular to the pressure gradient: $k^\perp = (\phi_1/k_1 + \phi_2/k_2)^{-1}$. The bound k^\parallel can also be attained, by stripes parallel to the pressure gradient: $k^\parallel = \phi_1 k_1 + \phi_2 k_2$. Physically, these special textures act like resistors in series and in parallel, respectively.

Using (2) and (3), the corresponding bounds for the effective slip length are

$$\frac{\langle \beta \rangle + 4\beta_1\beta_2}{1 + 4\langle \tilde{\beta} \rangle} \leq \beta^* \leq \frac{\langle \beta \rangle + \beta_1\beta_2}{1 + \langle \tilde{\beta} \rangle} \quad \text{case (I)} \quad (4a)$$

$$\frac{\langle \beta \rangle + 6\beta_1\beta_2}{1 + 6\langle \tilde{\beta} \rangle} \leq \beta^* \leq \langle \beta \rangle \quad \text{case (II)} \quad (4b)$$

where

$$\langle \beta \rangle = \phi_1\beta_1 + \phi_2\beta_2 \quad \text{and} \quad \langle \tilde{\beta} \rangle = \phi_2\beta_1 + \phi_1\beta_2 \quad (5)$$

are the average slip length and average transposed slip length, respectively. Using parameters for typical superhydrophobic surfaces, these bounds are plotted versus

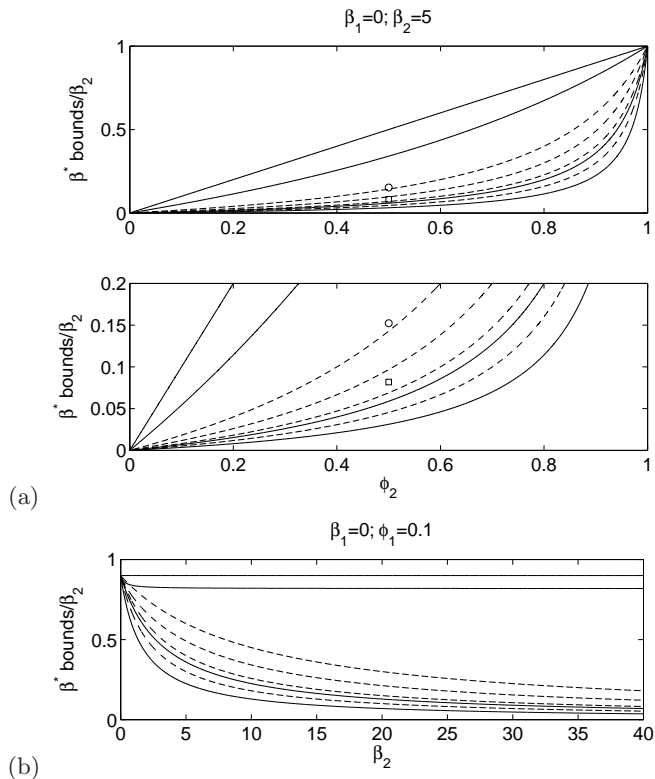


FIG. 2: (a) Bounds on the (normalized) superhydrophobic slip length β^*/β_2 versus the liquid-gas area fraction ϕ_2 , assuming no slip $\beta_1 = 0$ and high-slip $\beta_2 = 5$ on the liquid-solid and liquid-gas interfaces, respectively. Bottom: zoom of top figure. Dashed and solid lines correspond to cases (I) and (II) or one or two superhydrophobic surfaces, respectively. In each case, curves from top to bottom represent: the upper bound for anisotropic, upper bound for isotropic, lower bound for anisotropic textures. The value of β^* for the chessboard or the isotropic Schulgasser structure sketched in Fig. 3 is also shown (square: case (I), circle: case (II)). (b) The same bounds plotted versus the slip length β_2 for $\phi_2 = 0.9$.

the liquid-gas area fraction ϕ_2 in Fig. 2(a) and versus the liquid-gas slip length β_2 in Fig. 2(b). In case (I) the bounds are fairly close (especially when β_2 is large), so the theory provides a good sense of the possible effective slip of any texture, based only on the area fractions and local slip lengths. In case (II) the difference between the upper and lower bounds is larger and grows quickly with β_2 . In either case, however, the texture attaining the upper (lower) bound corresponds to stripes oriented parallel (transverse) to the pressure gradient [27].

Isotropic textures.— Consider now any isotropic structure, without a preferred direction ($\mathbf{k}^* = k^*\mathbf{I}$). If the only knowledge about the two-phase texture is ϕ_1, ϕ_2 , then the Hashin-Shtrikman (HS) bounds apply for the effective permeability, $k_{\text{HS}}^L \leq k^* \leq k_{\text{HS}}^U$, where (assuming

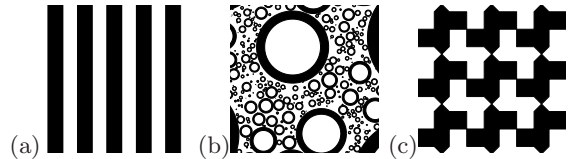


FIG. 3: Special textures arising in the theory: (a) stripes, which attain the Wiener bounds of maximal and minimal effective slip, if oriented parallel or perpendicular to the applied pressure gradient, respectively; (b) the Hashin-Shtrikman fractal pattern of circles, which attains the maximal slip among all isotropic textures; and (c) the Schulgasser texture, whose effective slip follows from the phase-interchange theorem.

$\beta_1 \leq \beta_2$ without loss of generality):

$$k_{\text{HS}}^L = \langle k \rangle - \frac{\phi_1 \phi_2 [k]^2}{\langle \tilde{k} \rangle + k_1}, \quad k_{\text{HS}}^U = \langle k \rangle - \frac{\phi_1 \phi_2 [k]^2}{\langle \tilde{k} \rangle + k_2}$$

with $[k] = k_2 - k_1$ and using the same notation as in (5). Using (2) and (3), the corresponding bounds for the effective slip length are obtained in a form similar to (4):

$$\frac{\langle \beta \rangle + f(\beta_1)\beta_1\beta_2}{1 + f(\beta_1)\langle \tilde{\beta} \rangle} \leq \beta^* \leq \frac{\langle \beta \rangle + f(\beta_2)\beta_1\beta_2}{1 + f(\beta_2)\langle \tilde{\beta} \rangle} \quad (6)$$

where

$$f(\beta) = \begin{cases} (5 + 3\beta)/(2 + 5\beta) & \text{case (I)} \\ 3/(1 + 3\beta) & \text{case (II)} \end{cases} \quad (7)$$

The HS bounds (6) are plotted in Fig. 2 in the same way as the Wiener bounds (4) and behave similarly, aside from being closer and confined between them. However, it turns out that isotropy does not dramatically reduce (enhance) the maximum (minimum) effective slip in a thin channel, especially in the configuration with two superhydrophobic surfaces, case (II).

The upper bound for isotropic textures can be attained by a fractal pattern of nested circular patches [25] as shown in Fig 3. It is interesting to note that similar patterns might be expected for a random (and sometimes fractal) nanobubble coating [28]. However, it is not necessary to deal with fractal surfaces: some periodic honeycomb-like structures also attain the bound [29].

Finally, we use phase interchange results [25] to obtain the effective slip length without any calculations, for a special class of isotropic textures. For a medium that is invariant by a $\pi/2$ rotation followed by a phase interchange, a classical result follows: $k^* = \sqrt{k_1 k_2}$. Examples of such media are the chessboard and the Schulgasser texture, sketched in Fig. 3(c). The effective β^* is then easily obtained from (3), although the corresponding values, shown in Fig. 2, are far from the HS upper bound.

Concluding remarks: design strategies— We close by proposing some guidelines for the design of thin superhydrophobic microchannels, which maximize effective

slippage, e.g. for lab-on-a-chip applications. We assume a principal direction of the texture is aligned with the side walls, since this is typically the fastest orientation. (Tilted textures also complicate analysis, since the constraint of no transverse flow, $\langle U \rangle_y = 0$, induces a transverse pressure gradient, $\langle \nabla p \rangle_y = -(k_{yx}^*/k_{yy}^*)\langle \nabla p \rangle_x$, which in turn affects the mean forward flow, $\langle U \rangle_x = -(1/\mu) \det(\mathbf{k}^*)/k_{yy}^*$ [13].) For simplicity, we also restrict now to the case $\beta_1 = 0$ of no-slip support structures.

It has been predicted for thick ($L \ll h$) cylindrical [16] and planar channels [17, 21] that the longitudinal stripe configuration has larger effective slip than the transverse one. For a thin channel ($L \gg h$), we can now draw the more general conclusion that longitudinal (transverse) stripes provide the largest (smallest) possible slip that can be achieved by any texture. Interestingly, this in contrast to a prediction for thick channels, where an array of pillars in the limit $\phi_2 \rightarrow 1$ has larger slip than longitudinal stripes [20].

We have shown that the key parameter determining effective slip is the area fraction of solid, ϕ_1 , in contact with the liquid. If this is very small (or $\phi_2 \rightarrow 1$), for all textures the effective slip tends to a maximum, $\beta^* \rightarrow \beta_2$. In this limit, the microchannel produces a kind of superfluidity, with plug-like flow. However, even a very small ϕ_1 is enough to reduce the effective slip significantly since in this limit (except an upper limit for case (II), where $\phi_2 - \beta^*/\beta_2 = 0$) we have the asymptotic scaling $\phi_2 - \beta^*/\beta_2 \propto \beta_2 \phi_1$. It is interesting that in case of perfect slip over the gas areas, β^* scales as $\propto \phi_2/\phi_1$, which is similar to an earlier result for a thick cylinder with transverse stripes [16]. For thin channels, we see now that this result is very general and is valid for any texture (and likely any channel geometry) with perfect slip patterns, representing “obstacles” to the flow. We thus conclude that in many situations, maximizing β_2 is not nearly as important as optimizing the texture to achieve large effective slip.

Finally, we have demonstrated that for all slip lengths and all fractions the largest possible β^* is equal to the area-averaged slip length $\langle \beta \rangle$, attained by longitudinal superhydrophobic stripes. However, for all textures the effective slip nearly coincide with the average, provided β_2 is small (or, more generally, $\beta_2 - \beta_1$ is small). Although this limit is less important for pressure-driven microfluidics, it may have relevance for amplifying transport phenomena [5].

In summary, we have connected the problem of effective slip over superhydrophobic surfaces in thin channels with the classical subject of conduction in heterogeneous media. This has allowed us to obtain rigorous bounds on slip for arbitrary textures and to obtain the slip in some cases without any calculations. Our results can be used to guide the design of superhydrophobic surfaces for thin micro- or nano-channels (where slip is most important), and some principles may hold for thick channels as well.

MZB and OIV gratefully acknowledge the hospitality of the ESPCI through Paris-Sciences and Joliot Chairs. OIV was partly supported by the DFG through its priority programme “Micro- and nanofluidics” (grant Vi 243/1-3).

-
- [1] D. Quere, Rep. Prog. Phys. **68**, 2495 (2005).
 - [2] J. Bico, U. Thiele, and D. Quere, Colloids Surfaces A **206**, 41 (2002).
 - [3] H. A. Stone, A. D. Stroock, and A. Ajdari, Annual Review of Fluid Mechanics **36**, 381 (2004).
 - [4] T. M. Squires and S. R. Quake, Reviews of Modern Physics **77**, 977 (2005).
 - [5] A. Ajdari and L. Bocquet, Phys. Rev. Lett. **96**, 186102 (2006).
 - [6] A. D. Stroock, S. K. W. Dertinger, A. Ajdari, I. Mezić, H. A. Stone, and G. M. Whitesides, Science **295**, 647 (2002).
 - [7] O. I. Vinogradova, Int. J. Mineral Proces. **56**, 31 (1999).
 - [8] E. Lauga, M. P. Brenner, and H. A. Stone, *Handbook of Experimental Fluid Dynamics* (Springer, NY, 2007), chap. 19, pp. 1219–1240.
 - [9] L. Bocquet and J. L. Barrat, Soft Matter **3**, 685 (2007).
 - [10] O. I. Vinogradova, Langmuir **11**, 2213 (1995).
 - [11] A variant of this picture is a nanobubble-coated hydrophobic surface [28, 30].
 - [12] O. I. Vinogradova and G. E. Yakubov, Langmuir **19**, 1227 (2003).
 - [13] M. Z. Bazant and O. I. Vinogradova, J. Fluid Mech. (2008), in press.
 - [14] P. Joseph, C. Cottin-Bizon, J. M. Benoit, C. Ybert, C. Journet, P. Tabeling, and L. Bocquet, Phys. Rev. Lett. **96**, 156104 (2006).
 - [15] J. Ou and J. P. Rothstein, Phys. Fluids **17**, 103606 (2005).
 - [16] E. Lauga and H. A. Stone, J. Fluid Mech. **489**, 55 (2003).
 - [17] C. Y. Wang, Physics of Fluids **15**, 1114 (2003).
 - [18] M. Sbragaglia and A. Prosperetti, Phys. Fluids **19**, 043603 (2007).
 - [19] A. A. Alexeyev and O. I. Vinogradova, Colloids Surfaces A **108**, 173 (1996).
 - [20] C. Ybert, C. Barentin, C. Cottin-Bizonne, P. Joseph, and L. Bocquet, Physics of Fluids **19**, 123601 (2007).
 - [21] C. Cottin-Bizonne, C. Barentin, E. Charlaix, L. Bocquet, and J. L. Barrat, Eur. Phys. J. E **15**, 427 (2004).
 - [22] N. V. Priezjev, A. A. Darhuber, and S. M. Troian, Phys. Rev. E **71**, 041608 (2005).
 - [23] R. Benzi, L. Biferale, M. Sbragaglia, S. Succi, and F. Toschi, J. Fluid Mech. **548**, 257 (2006).
 - [24] K. Z. Markov, in *Heterogeneous Media, Modelling and Simulation*, edited by K. Markov and L. Preziosi (Birkhauser Boston, 2000), chap. 1, pp. 1–162.
 - [25] S. Torquato, *Random Heterogeneous Materials: Microstructure and Macroscopic Properties* (Springer, 2002).
 - [26] J. Hyväluoma and J. Harting, Phys. Rev. Lett. **100**, 246001 (2008).
 - [27] This raises interesting questions about correlations between an effective slip and static wetting properties (contact angle) of the wall [31]. For example, in the stripe

- geometry the “transverse” contact angle is larger than “parallel” [32], which is opposite to trends in slippage.
- [28] O. I. Vinogradova, N. F. Bunkin, N. V. Churaev, O. A. Kiseleva, and B. W. Ninham, *J. Colloid Interface Sci.* **173**, 443 (1995).
- [29] S. Torquato, L. Gibiansky, M. Silva, and L. Gibson, *Int. J. Mech. Sci.* **40**, 71 (1998).
- [30] B. M. Borkent, S. M. Dammler, H. Schönherr, G. J. Vansco, and D. Lohse, *Phys. Rev. Lett.* **98**, 204502 (2007).
- [31] R. S. Voronov, D. V. Papavassiliou, and L. L. Lee, *Ind. Eng. Chem. Res.* **47**, 2455 (2008).
- [32] J. Bico, C. Marzolin, and D. Quere, *Europhys. Lett.* **47**, 220 (1999).